

Mesenchymal cells from adult kidney support angiogenesis and differentiate into multiple interstitial cell types including erythropoietin-producing fibroblasts

Matthew D. Plotkin and Michael S. Goligorsky

Renal Research Institute, New York Medical College, Valhalla, New York

Submitted 5 October 2005; accepted in final form 11 April 2006

Plotkin, Matthew D., and Michael S. Goligorsky. Mesenchymal cells from adult kidney support angiogenesis and differentiate into multiple interstitial cell types including erythropoietin-producing fibroblasts. *Am J Physiol Renal Physiol* 291: F902–F912, 2006. First published April 18, 2006; doi:10.1152/ajprenal.00396.2005.—Mesenchymal cells have been isolated from embryos and multiple adult organs where they may differentiate into various connective tissue cell types and provide paracrine support for surrounding cells. With the use of a technique for culturing multipotent mesenchymal cells from adult tissues, a fibroblast-like cell clone (4E) was isolated from adult mouse kidney. 4E cells were able to differentiate along multiple mesodermal lineages including cell types located in the renal interstitium such as fibroblasts and pericytes. Coculture of 4E cells with ureteric bud and epithelial cell lines and analysis of resulting changes in gene expression revealed that these cells support angiogenesis and tubulogenesis and expressed genes characteristic of embryonic renal stromal cells. Following subcapsular injection after unilateral ischemia-reperfusion in adult mice, 4E cells migrated to a peritubular interstitial location and expressed interstitial cell markers, whereas cells injected in control kidneys remained stationary. Incubation in hypoxic or anoxic conditions resulted in erythropoietin expression in a small subset of ecto-5'-nucleotidase-positive cells and resulted in increased vascular endothelial growth factor expression in the same cell population. Our findings suggest that the adult kidney may contain interstitial mesenchymal cell progenitors with embryonic stromal cell characteristics that are able to provide paracrine support for surrounding vessels and tubular epithelial cells and differentiate into erythropoietin producing fibroblasts.

fibroblast

MESENCHYMAL CELLS ARE CHARACTERIZED by their fibroblast-like morphology, extension of filopodia, and invasive motility (11). During embryonic development, they are derived from epithelial-to-mesenchymal transformation (EMT) and provide the fibroblasts, connective tissue, and extracellular matrix that model the developing tissue. Following migration to target areas throughout the embryo, these cells differentiate into numerous cell types including osteoblasts, smooth muscle, endothelial cells, adipocytes, and chondrocytes and/or induce differentiation of other cells through production of matrix proteins and paracellular signaling factors (11). In the adult, mesenchymal cells are located within the interstitium or stroma of all organs and retain at least part of their embryonic plasticity. In these organs, mesenchymal cells may serve as fibroblast precursors that provide the extracellular matrix and cytokines necessary for epithelial homeostasis and regenera-

tion and repair following injury (33). Mesenchymal cells can be easily cultured from adult tissues using various methods that are based on cell adherence to a solid surface. Numerous in vitro studies demonstrated their potential to mediate repair of injured tissue. A trophic or support role for bone marrow mesenchymal cells infused following kidney injury has also been shown (38). Whether a population of resident mesenchymal or stromal cells with similar characteristics exists within the adult kidney interstitium that can support kidney repair remains unknown.

Despite increasing knowledge about the origin and differentiation of kidney epithelial cells, little is known about the differentiation of the various renal interstitial cell types. During embryogenesis, the kidney contains a population of mesenchymal cells that form a stroma surrounding developing tubules and glomeruli. These stromal cells express a unique set of transcription factors and secrete growth factors responsible for nephron induction and differentiation (5). These cells subsequently form the interstitium of the adult kidney that includes various cell types such as cortical and medullary fibroblasts, endothelium, pericytes, and dendritic cells (2). After kidney injury, interstitial cells provide support for epithelial repair and may assume an immature phenotype, recapitulating their role during development (12). Based on studies from other tissues, mesenchymal cells isolated from adult kidney may be closely related to or identical to stromal cells identified during development and therefore reside within the peritubular interstitial space.

With the use of a method developed for culture of mesenchymal cells from skeletal muscle and bone marrow (39), a fibroblast-like cell line with embryonic kidney stromal characteristics was isolated from adult mouse kidney. The following results demonstrate that these fibroblast-like cells are able to support angiogenesis and in vitro tubulogenesis and express many of the genes important for stromal cell function during development. In response to hypoxia, these cells increase production of vascular endothelial growth factor (VEGF) and express erythropoietin (EPO). Evidence is presented that these cells may be useful for further studies of renal stromal cell differentiation, factors affecting renal EPO production and mesenchymal-epithelial and endothelial interactions that may be important for normal kidney homeostasis and repair.

METHODS

Isolation and culture of mouse kidney mesenchymal cells. Cells were isolated from kidneys of 2-mo-old female FVB/NJ mice trans-

Address for reprint requests and other correspondence: M. Plotkin, New York Medical College Renal Research, BSB C06, 95 Grasslands Rd., Valhalla, NY 10595 (e-mail: matthew_plotkin@nyc.edu).

The costs of publication of this article were defrayed in part by the payment of page charges. The article must therefore be hereby marked "advertisement" in accordance with 18 U.S.C. Section 1734 solely to indicate this fact.

genic for green fluorescent protein (GFP) linked to the Tie-2 promoter (26) using a protocol developed by Young et al. (21). Mice were treated according to the National Institutes of Health *Guide for the Care and Use of Laboratory Animals*. Kidneys were minced and digested with collagenase (250 U/ml) and dispase (33.3 U/ml) at 37°C to a single-cell suspension and plated on 1% gelatin-coated dishes in EMEM (Invitrogen, Carlsbad, CA) with 10% preselected horse serum (Gem Biotech, Woodland, CA) plus antibiotics. Nonadherent cells were removed after 48 h. Following confluence, cells were filtered through a 20- μ m Nitex filter and slowly frozen to -80°C in 7.5% DMSO. Cells were thawed and grown to confluence. The freeze-thaw cycle was repeated to further remove remaining differentiated cell types as described (39). Individual cell clones were isolated using cloning cylinders and grown to confluence. Serum-free medium consisted of DMEM/F12 (Invitrogen) with insulin, transferrin and selenium, hydrocortisone (10^{-9} M), thyroxine (10^{-9} M), PGE₁ (25 ng/ml; Sigma, St. Louis, MO), and TGF- α (5 ng/ml; Peprotech, Rocky Hill, NJ).

Hypoxic cells were cultured in 2% O₂ with 5% CO₂ and 93% N₂ using a controlled atmosphere chamber and O₂ analyzer (ProOx 110, Reming Bioinstruments, Redfield, NY). Anoxic cells were cultured using BBL GasPak anaerobic pouches (BD, San Diego, CA).

Analysis of surface antigen expression by flow cytometry. Cell surface antigen expression was analyzed with a FACSCalibur machine (BD); 1×10^5 cells in PBS with 2% FBS (Invitrogen) and 0.01% NaN₃ were incubated for 30 min at room temperature with PE-conjugated antibodies (BD) against Sca-1, CD34, c-Kit, Flk-1, and CD45. Control cells were labeled with PE-conjugated isotype-specific antibodies at equal concentration. Data analysis was performed with Cell Quest software. Each analysis included at least 5,000 events and was performed on cells from at least three separate preparations.

In vitro differentiation assays and use of recombinant cytokines and growth factors. Confluent cells were grown in serum-free medium with addition of the following cytokines and growth factors: recombinant murine N-Sonic hedgehog (Shh; R & D Systems, Minneapolis, MN), recombinant murine FGF-2 (50 ng/ml), and TGF- β 1 (5 ng/ml; Peprotech). For coculture with rat ureteric bud (RUB-1) cells (gift of Dr. A. Perantoni), cultures were grown in serum-free medium as previously described (26).

Immunofluorescent and immunohistochemical staining. Cells were fixed with 4% paraformaldehyde or methanol at -20°C for 10 min. Immunohistochemical staining was performed using a DAB-streptavidin kit (Dako, Carpinteria, CA) according to the manufacturer's instructions. Immunofluorescence was performed by blocking cells with 10% goat serum and 0.1% Tween 20 in PBS followed by incubation with primary antibodies overnight at 4°C. Following washes with PBS, cells were incubated with FITC or Texas red-conjugated goat secondary antibodies (Jackson ImmunoResearch, West Grove, PA). Primary antibodies used were: mouse monoclonal anti- α smooth muscle actin (1:250; clone 1A4, Dako), goat polyclonal anti-CD31 (1:100; Santa Cruz Biotechnology, Santa Cruz, CA), rat monoclonal MOMA-2 (1:50; Serotec, Raleigh, NC), mouse monoclonal anti-calponin (1:100; clone hCP, Sigma), monoclonal anti-vimentin (1:100; clone LN-6, Sigma), rabbit polyclonal anti-Flk-1 (1:100; Santa Cruz Biotechnology), goat polyclonal anti-Flt-1 (1:100; Santa Cruz Biotechnology), rabbit polyclonal anti-EPO (1:100; Santa Cruz Biotechnology), rabbit polyclonal anti-ZO1 (1:100; Zymed, Carlsbad, CA), mouse monoclonal anti-pan cytokeratin clone (1:100; Sigma), rat monoclonal anti-tenascin (1:100; clone MTN-12, Sigma), rat monoclonal anti-5'-NT (1:50; BD), and rabbit polyclonal anti-S100A4 (1:100; Dako). Control sections were labeled without primary antibody and addition of normal goat or rabbit IgG.

RNA isolation and semiquantitative PCR. Total RNA was isolated from cells using RNeasy Mini Columns (Qiagen, Valencia, CA) according to the manufacturer's instructions. RNA was DNase-1 treated with an on-column system to remove residual genomic DNA. cDNA was prepared from 2 μ g of RNA with AMV reverse transcrip-

tase (Roche, Indianapolis, IN). Semiquantitative PCR was performed using 18S RNA internal standards (Ambion, Austin, TX) using cycle numbers previously determined to amplify products within the linear range. The following PCR primers were used for amplification: VEGF receptor 2 (Flk-1) forward 5'-AGAACA CCAAAA GAGAGGAACG and reverse GCACACAGGCAGAAACCAG TAG-3', Pod-1 forward 5'-AGGAGTTTGGAACTTCCAACGAGA-3' and reverse 5'-TCTCGTACTTGTCTGTTGGC CAGGA-3', retinoic acid receptor b2 forward 5'- GATTCTGGGCTGGGAAAAAG-3' and reverse 5'-CGGTGTAGAAATCCA GGATC-3', patched forward 5'-CTCAGCAATACGAAGCACA-3' and reverse 5'-GACAAG-GAGCCAGAGTCCAG-3', BMP4 forward 5'-TGTGAGGAGTTTC-CATCAG-3' and reverse 5'-TTATTCTTCTTCTGACCG-3', EPO forward 5'-GAGGCAGAAAATGTCACGATG-3' and reverse 5'-CTTCCACCTCCATTCTTTTCC-3', BF-2 forward 5'-TATGCT-GCAACCCCTGACTTG-3' and reverse 5'-AAACGCTGGACCTGT-GAATC-3', PDGF β R forward 5'-AGCTACATGGCCCCCT-TATGA-3' and reverse 5'-GGATCCCAAAGACCAGACA-3'.

Western blot analysis. Cells were lysed with RIPA buffer (20 mM Tris, pH 7.8, 140 mM NaCl, 1 mM EDTA, 1% Triton X-100, 0.1% SDS, 1% sodium deoxycholate, 1 mM NaF, and 1 mM orthovanadate) with Complete Mini protease inhibitors (Roche). Protein concentration was determined using a Bradford assay (Bio-Rad, Hercules, CA). Equal amounts of protein were separated in 4–20% Tris-glycine gels (Invitrogen) and transferred to Immobilon-P membranes (Millipore, Bedford, MA). Following blocking with PBS/5% nonfat dry milk, membranes were incubated with the following primary antibodies: mouse monoclonal anti-Calponin (1:2,000; Sigma), mouse monoclonal β -tubulin and β -actin (1:3,000; Sigma), goat polyclonal anti-erythropoietin (1:700; R&D Systems), goat polyclonal anti-CD31 (1:200; Santa Cruz Biotechnology), rat monoclonal MECA-32 (1:300; Developmental Hybridoma Bank), rat anti-mouse tenascin (1:300; Sigma), rabbit polyclonal anti-VEGFA (1:250; Santa Cruz Biotechnology), and goat polyclonal anti-Pod-1 (1:200; Santa Cruz Biotechnology). Following washes with PBS/0.1% Tween 20, membranes were incubated with horseradish peroxidase-conjugated secondary antibodies (Amersham, Piscataway, NJ) for 60 min at room temperature. Membranes were washed and protein was detected by Super-Signal West Pico chemiluminescence (Pierce, Rockford, IL).

Subcutaneous matrigel implant angiogenesis assays. Cells were labeled with DiI Cell-Tracker (Invitrogen/Molecular Probes) according to the manufacturer's instructions and 5×10^5 cells were suspended in 0.5 ml growth factor reduced Matrigel (BD) with 50 μ g/ml heparin and injected subcutaneously into the abdominal wall of anesthetized FVB/NJ adult male mice, $n = 3$, ages 2–4 mo. Control animals, $n = 3$, were injected with Matrigel and heparin alone. After 10 days, Matrigel plugs were removed and processed for immunohistochemistry using frozen sections as described above.

Subcapsular cell injection following kidney ischemia-reperfusion. Male FVB/NJ mice (aged 2–4 mo), $n = 6$, were anesthetized with ketamine and xylazine and subjected to 45 min of left unilateral kidney ischemia using a microvascular clamp; 0.5×10^6 DiI labeled 4E cells suspended in PBS were injected under the capsule of both ischemic and contralateral control kidneys. Following clamp removal, reperfusion of the kidneys was visually confirmed. Kidneys were removed 7 days after surgery following perfusion fixation with 4% paraformaldehyde via the left ventricle. Cryostat sections were stained as described above.

Cell proliferation assays. Cells were seeded at equal density in 96-well plates and cultured with BrdU overnight. BrdU incorporation was measured using an ELISA kit (Roche) according to the manufacturer's instructions. Colorimetric signal (A_{450}) was measured using a Bio-Tek EL800 plate reader. Statistical differences between two groups were determined using Student's *t*-test.

VEGF ELISA. Subconfluent cells were grown in control (21% O₂ and 5% CO₂) and hypoxic (2% O₂, 5% CO₂, and 93% N₂) conditions for 48 h. Protein extracts were prepared as described above. Equal

amounts of protein were diluted in buffer (PBS, 0.1% BSA, 0.05% Tween 20) and VEGF concentration was measured using a mouse VEGF ELISA kit (Peprotech) that recognizes the 120- and 164-kDa isoforms of VEGFA. VEGF concentrations were determined using a standard curve prepared with each experiment. Results represent pooled data from three independent experiments.

EPO ELISA. EPO protein concentrations in cell lysates and culture supernatant from control and hypoxia-treated cultures were measured using a mouse EPO ELISA kit (Quantikine, R&D Systems) according to the manufacturer's instructions. The mean minimum detectable dose of mouse EPO was 18 pg/ml as determined by the manufacturer. Results represent pooled data from two independent experiments.

RESULTS

Isolation and characterization of renal mesenchymal cells. Cells were cultured from kidneys of adult Tie2-GFP transgenic FVB/NJ mice using a technique for isolating multipotent mesenchymal cells from muscle and bone marrow (21). The isolation procedure has been used to culture cells with mesenchymal characteristics from both FVB and C57 mouse strains and typically yields 10–20 colonies from $2-3 \times 10^5$ cultured cells. The phenotype and gene expression profile of these cells were consistent across different animals with variation noted in the level of smooth muscle markers. Endothelial cells in these mice express GFP under control of the angiopoietin receptor Tie2 promoter, providing a fluorescent marker for the endothelial lineage. Single-cell clones were isolated using cloning cylinders and expanded. One clone (4E) was selected for further analysis based on mesenchymal or stromal cell characteristics and was used in all experiments described in this study. Cytogenetic analysis of 4E cells from *passage 21* showed that cultures contained a mixture of cells with a diploid or tetraploid chromosome number with no detectable chromosomal abnormalities by banding. Analysis of telomerase activity using a telemetric repeat amplification protocol (TRAP) showed that 4E cells retained enzyme activity at *passage 21* (data not shown). Expression of surface antigens, growth factor receptors, cytoskeletal proteins, and transcription factors was evaluated by FACS analysis, PCR, Western analysis, and immunocytochemistry (Table 1) and revealed a pattern characteristic of both mouse mesenchymal stem cells (MSC) and renal stromal progenitor cells (3, 5, 20, 28) including expression of Sca-1, CD44, CD34, and transcription factors Pod-1, BF-2, and receptors for sonic hedgehog, BMP and retinoic acid, respectively. 4E cells consistently expressed these markers between *passages 10* and *25* with no apparent loss of expression with increasing passage number.

To determine whether 4E cells maintain the multilineage differentiation potential characteristic of mesenchymal cells, cells from *passages 10-25* were cultured on gelatin-coated dishes with cytokines known to induce cell differentiation and labeled with phenotype specific markers (Fig. 1). Undifferentiated cells maintained a dendritic cell-like morphology with extension of numerous filopodia (Fig. 1A), ranged in size from ~10 to 20 μm and expressed the mesenchymal cell marker vimentin. Adipocytes were induced in cultures grown at low density in serum-free medium with 10^{-9} M hydrocortisone for 2 wk (Fig. 1B). Following treatment with TGF- β_1 for 3 days, all cells expressed α -smooth muscle actin consistent with smooth muscle or myofibroblast differentiation (Fig. 1C). Osteoblasts were identified by Von Kossa's stain for calcified

Table 1. 4E cell expression profile of \dagger MSC and *stromal markers

Phenotype Marker	Expression (% Cells)	Method(s) Used to Identify
Surface antigen		
Sca-1 \dagger	+ (100)	FACS, W
CD34 \dagger	+ (100)	FACS
CD44 \dagger	+ (100)	IC
CD73 (5'-NT)	+ (<10)	IC
CD45	–	FACS
c-Kit	–	FACS
Receptor (ligand)		
Flk-1 (VEGF)	+ (<10)	FACS, IC, PCR
Patched (Sonic hedgehog)*	+	PCR
Retinoic acid α *	+	PCR
PDGF β *	+	W, IC, PCR
BMP4*	+	PCR
CXCR4 (SDF-1)*	+	PCR
Cytoskeleton protein		
Vimentin*	+ (100)	IC
Cytokeratin	–	IC
Nestin	+	W, IC
Transcription factor		
Pod-1*	+	PCR, W
BF-2*	+	PCR
WT-1	–	PCR

W, Western blot; IC, immunocytochemistry.

matrix (Fig. 1D) and antibody to bone sialoproteins I and II (Fig. 1E, arrow and F) following growth in medium with ascorbic acid-2-phosphate and β -glycerolphosphate for 2 wk. Endothelial cells were induced by growth on type IV collagen in serum-free medium for 1 wk and identified by expression of VEGF receptor 2 (Flk-1; Fig. 1G) and coexpression of GFP from the Tie2 promoter (Fig. 1H) and expression of VEGF receptor 1 (Flt-1, arrows; Fig. 1I). Following culture at low density in 10% FBS for 1 wk, a small number of macrophages identified by MOMA-2 staining, a marker for an intracellular mouse macrophage, and monocyte antigen (19) were also detected (Fig. 1J). The differentiation potential of 4E cells remained the same across *passages 10-24*. In all studies, undifferentiated cells were completely negative for the differentiation markers described, with the exception of a subset of cells that expressed α -smooth muscle actin. The TGF- β induction of smooth muscle-specific gene expression was confirmed by Western analysis of the contractile proteins sm22 α and calponin (Fig. 2A) and induction of the endothelial marker Flk-1 was confirmed by RT-PCR in control and treated cells (Fig. 2B). 4E cells did not express the epithelial protein cytokeratin by immunocytochemistry or Western analysis and no evidence for differentiation into cells of endodermal or ectodermal germ cell lineages was observed using hepatocyte and glial markers, respectively (not shown).

Matrigel angiogenesis assay using renal mesenchymal cells. Because 4E cells expressed endothelial markers in vitro, an in vivo subcutaneous Matrigel implant assay (27) was used to determine whether 4E cells can participate in angiogenesis. 4E cells were labeled with the fluorescent dye DiI and suspended in growth factor reduced Matrigel. Matrigel was injected subcutaneously into wild-type FVB/NJ mice and removed after 10 days for histological examination. Matrigel plugs containing 4E cells demonstrated a dense growth of capillary vessels stained with anti-CD31 antibody, an endothelial cell marker (Fig. 3A, low-power, and 3C, high-power magnification). In

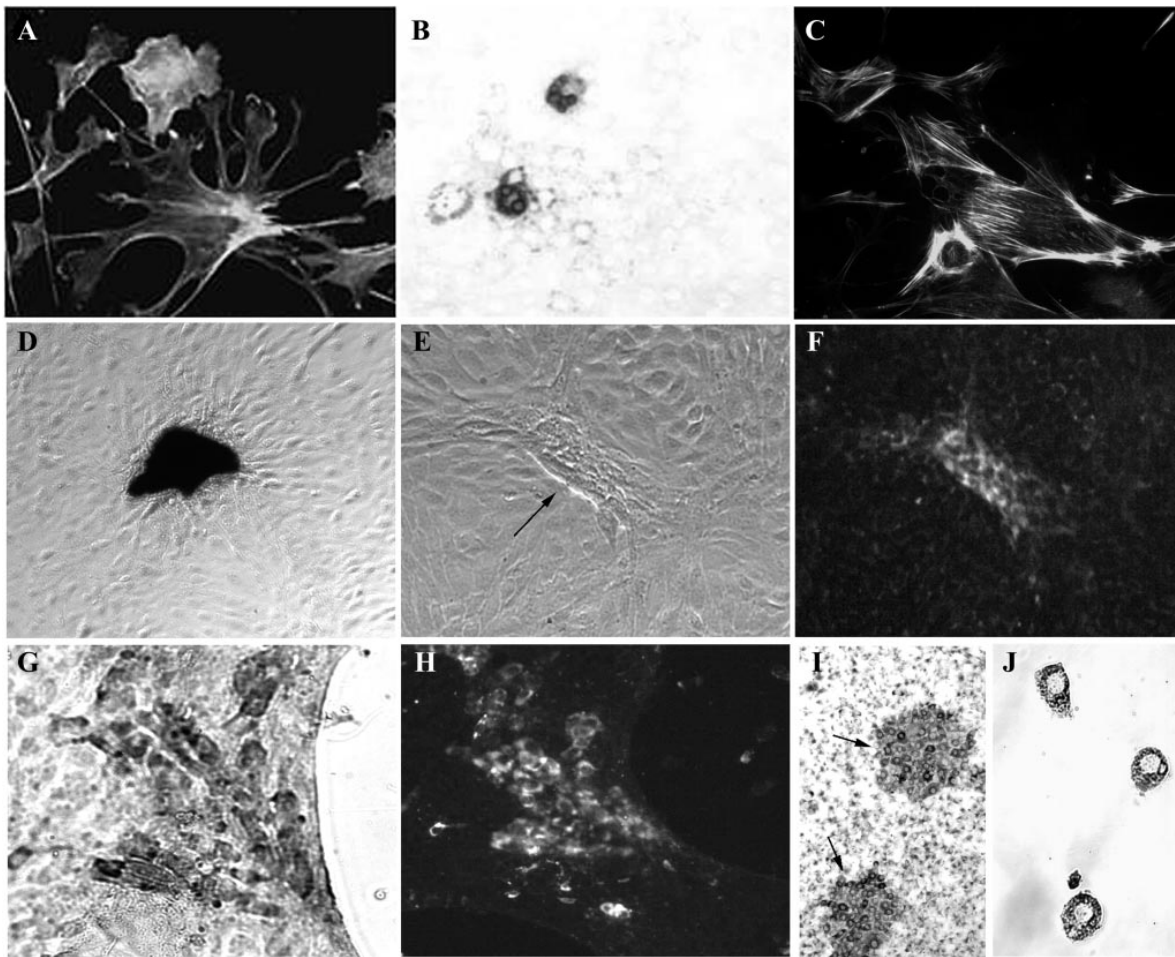


Fig. 1. In vitro differentiation of 4E cells into multiple phenotypes. *A*: Texas red-phalloidin staining of undifferentiated cells. *B*: adipocytes stained with oil red O. *C*: α -smooth muscle actin expression following TGF- β (5 ng/ml) in serum-free medium for 3 days. *D*: osteoblasts identified by Von Kossa's stain for calcified matrix and antibody to bone sialoproteins I and II [*E*, phase image (arrow), *F*, immunofluorescence]. Endothelial cells identified by expression of VEGFR2/Flk-1 (*G*) and coexpression of Tie2-GFP (*H*) and expression of VEGFR1/Flt-1 in clusters (arrows, *I*). *J*: macrophage differentiation detected by MOMA-2 staining. Original magnification $\times 100$.

contrast, plugs without 4E cells demonstrated a nearly 10-fold reduction in capillary growth (Fig. 3*D*) with only a small number of peripheral capillary sprouts detected (Fig. 3*B*). Double fluorescence images of DiI-labeled 4E cells (Fig. 3*E*, red) showed that many cells were also Tie2-GFP positive (Fig. 3*F*, green), consistent with endothelial differentiation. Immunolabeling for CD31 to detect recipient endothelial cells revealed that capillary structures were formed by a mixture of cells including DiI, GFP/CD31-negative 4E cells (Fig. 3*G*, red), DiI negative, CD31-positive recipient endothelial cells (green), and double positive 4E cells expressing endothelial markers (yellow). Additional evidence for 4E pericyte differentiation was obtained by coculture of DiI-labeled 4E cells with HUVEC cells; 24-h cocultures on Matrigel demonstrated 4E cell apposition along HUVEC capillary networks labeled with UEA-I lectin (Fig. 3*H*). Coculture induced expression of the PDGF β receptor (Fig. 3*J*) in 4E cells, characteristic of pericytes, an effect also seen by Western blot analysis (Fig. 3*J*)

showing a fivefold increase in protein level. Together, these results demonstrate that 4E cells are capable of producing capillary structures by differentiation into endothelial cells and pericytes.

Coculture with rat ureteric bud cell. Reciprocal interactions between the ureteric bud and surrounding mesenchyme result in differentiation and morphogenesis of the developing kidney. To determine whether 4E cells differentiate in response to inductive signals that may regulate stromal cell differentiation during development, cells were cocultured with RUB1 cells, a ureteric bud cell line that has been shown to secrete factors that induce differentiation and morphogenesis of metanephric mesenchyme (16). Results from experiments using cocultures of equal numbers of DiI-labeled 4E and RUB1 cells grown in direct contact in serum-free medium for 1 wk are shown in Fig. 4. Aggregates of 4E cells formed after 1 wk of coculture (Fig. 4*A*, arrows). Cell aggregates demonstrated faint GFP signal indicating no significant Tie2 expression. Immunostaining of

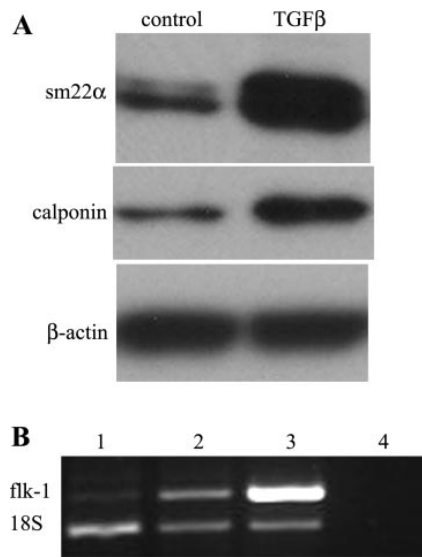


Fig. 2. Induction of smooth muscle and endothelial-specific gene expression in 4E cells. Cells were grown in control and inducing conditions as previously described. **A:** Western analysis of sm22 α and calponin expression with β -actin loading control. **(B)** RT-PCR with 18S internal control. *Lane 1:* undifferentiated cells. *Lane 2:* 1-wk growth in serum-free medium on type IV collagen. *Lane 3:* whole mouse embryo-positive control. *Lane 4:* no RT.

DiI-labeled 4E cell aggregates for the endothelial marker Flk-1 demonstrated expression in cocultured cells (Fig. 4D) compared with no expression in 4E cells cultured in serum-free medium alone (Fig. 4C). Western blot analysis for endothelial markers CD31 and MECA-32 demonstrated induction in 4E cells by RUB1 coculture compared with control serum-free cultures where no expression was detected (Fig. 4G). Induction of calponin expression, a smooth muscle cell-specific cytoskeletal binding protein, was also seen along the periphery of 4E aggregates (Fig. 4F) with no expression in 4E cells cultured in serum-free medium alone (Fig. 4E). These markers colocalized with DiI-labeled 4E aggregates only and were not expressed in surrounding RUB1 cells. 4E aggregates expressed the matrix protein tenascin-C, a substratum for angiogenesis and mesenchymal cell differentiation (15) (Fig. 4H). No tenascin expression was seen in 4E cells cultured in serum-free medium alone (Fig. 4G). These results were confirmed by Western blot analysis (Fig. 4J). Coculture with RUB1 cells induced detectable levels of tenascin protein while addition of TGF- β ₁, an inducer of mesenchymal cell tenascin expression (9), had an effect equal to growth in serum but less than coculture with RUB1 cells while no expression was detected in cells grown in serum-free medium.

Coculture with Madin-Darby canine kidney cells. During embryonic nephrogenesis, stromal cells within the metanephric mesenchyme induce tubule elongation and differentiation through paracrine mechanisms. To examine potential paracrine effects of 4E cells on tubule formation, cells were cocultured with Madin-Darby canine kidney (MDCK) cells, a canine distal tubule cell line, using three-dimensional (3-D) type 1 collagen gels, a standard assay for *in vitro* tubulogenesis (25). Figure 5 demonstrates that when 4E cells were mixed with MDCK cells in a 1:2 ratio in 3-D gels, elongated PAS-positive

(Fig. 5A, *inset* arrowhead) tubular structures that expressed the tight junction protein ZO-1 (Fig. 5C, arrows and *inset*, arrows) were detected. In the absence of 4E cells, MDCK cells formed numerous cysts (Fig. 5B) that expressed ZO-1 on their inner surface (Fig. 5D). Coculture of DiI-labeled 4E cells with MDCK cells demonstrated that all tubular cells were DiI negative and therefore composed only of MDCK cells (data not shown).

Subcapsular injection of mesenchymal cells following renal ischemia-reperfusion. Recent studies demonstrated that bone marrow-derived mesenchymal stem cells migrate to the interstitium of injured kidneys where they may support repair and regeneration of injured tubules through paracrine effects and replace endothelial cells of injured vessels (6, 38). To test the ability of 4E cells to respond to and participate in renal repair *in vivo* by migration and incorporation into surrounding tissue, DiI-labeled cells were injected into the subcapsular area of kidneys injured with ischemia-reperfusion. The contralateral nonischemic kidney was also injected to serve as a control. Seven days after injury, kidneys were removed and analyzed for the location and phenotype of labeled cells. Representative images of kidneys from six mice are shown in Fig. 6. In control kidneys, labeled 4E cells were seen only in a subcapsular location without detectable migration (Fig. 6, A and B). In contrast, cells injected in ischemic kidneys appeared to migrate throughout the cortex and medulla, reaching as far as the papillary epithelium (Fig. 6, C-F). While the majority of injected cells remained close to the injection site in the outer cortex, ~10% of cells per section were located in the inner cortex or outer medulla. Cells were present in a peritubular interstitial location without evidence of incorporation into tubules or glomeruli. Most cells were located alongside peritubular capillaries identified with the endothelial marker CD31 (Fig. 6C). A small number of peritubular cells were α -smooth muscle actin positive (Fig. 6D). Cells that migrated to the papillary epithelium expressed type IV collagen (Fig. 6E), a major component of kidney epithelial basement membranes secreted by peritubular interstitial cells.

EPO and VEGF expression in response to hypoxia. Because 4E cells were capable of fibroblast differentiation and peritubular fibroblasts are the renal EPO producing cell (23), expression of EPO was examined in both control conditions and in response to anoxia and hypoxia. Using RT-PCR with cDNA prepared from subconfluent control cells and cells grown in anoxic (<1% O₂) and hypoxic (2% O₂) environments, EPO gene expression was not detectable under normoxic conditions but was clearly detectable after 24-h exposure to anoxia and at a lower level after 48 h of hypoxia (Fig. 7A). Cell lysates were prepared for EPO protein detection using both Western analysis and ELISA. Western blot analysis (Fig. 7B) revealed protein bands at 30 and 36 kDa in anoxic cells, corresponding to the nonglycosylated and glycosylated forms of mouse EPO, respectively. These bands were not detected in control normoxic cells. An additional band at 34 kDa was detected in both conditions and may be nonspecific. By ELISA, EPO protein was detectable in cell lysates of anoxic cells while no protein was detectable in control cells (Table 2). No EPO protein was detectable in nonconcentrated cell culture supernatants from both culture conditions.

To identify additional characteristics of the EPO-expressing 4E cells, cells grown in anoxic conditions for 24 h were

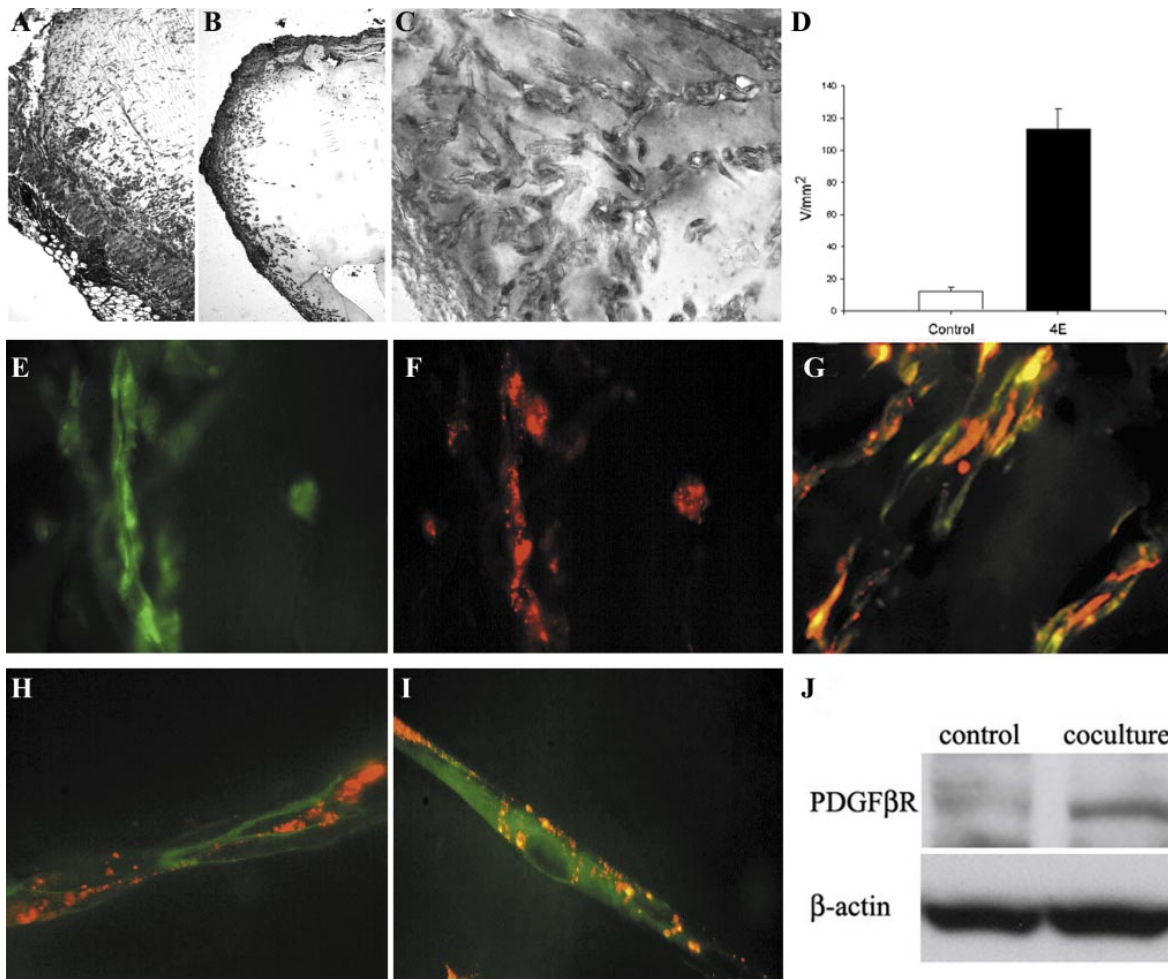


Fig. 3. Subcutaneous Matrigel (MG) angiogenesis assay and 4E cell pericyte differentiation in HUVEC cocultures. *A*: CD31 labeled MG plug with 4E cells demonstrating dense capillary formation. *B*: plugs without 4E cells contained few capillary sprouts at the gel periphery. *C*: high-power magnification of CD31 labeled capillaries in MG plug containing 4E cells. *D*: MG plugs with 4E cells contained a nearly 10-fold increase in capillary density. *E*: DiI (red)-labeled 4E cells co-expressing Tie2-GFP (*F*), consistent with endothelial differentiation. *G*: double fluorescence image of DiI-labeled 4E cells (red) and CD31 (green). 4E cells expressing CD31 are yellow and recipient endothelial cells are green. *H*: coculture of DiI-labeled 4E cells with HUVEC cells (UEA-1 lectin labeled, green) on MG for 24 h demonstrating 4E (red) apposition to endothelium. Expression of PDGFβ receptor (*I*, green, yellow) by 4E cell adherent to unlabeled HUVEC cell characteristic of pericyte phenotype. *J*: Western blot analysis with β-actin loading control demonstrating a 5-fold increase in PDGFβR protein level in expression in cocultured 4E cells. Original magnification $\times 40$ (*A*, *B*) and $\times 400$ (*C*, *E-I*).

immunolabeled for EPO and mesenchymal cell markers. EPO labeling was detected in cytoplasmic granules at low levels in $\sim 50\%$ of nonconfluent cells and was detected at substantially higher levels in less than 1% of cells (Fig. 7C). EPO expressing cells were α -SMA negative (Fig. 7D) and vimentin positive (Fig. 7H) while EPO-negative cells were both α -SMA and vimentin positive, characteristic of myofibroblasts. Anoxic conditions resulted in marked reduction in α -SMA expression compared with control conditions (Fig. 7E). Double labeling with anti-ecto-5'-nucleotidase (5'-NT) antibody, a renal cortical fibroblast marker expressed in EPO producing cells in vivo, revealed that most cells with increased EPO signal also expressed membrane 5'-NT (Fig. 7, *F* and *G*). Labeling with anti-FSP-1/S100A4 (Fig. 7H), a widely used marker for tissue fibroblasts and cells derived from EMT in the kidney following

injury (14), resulted in few positive cells ($<1\%$). Despite increased growth factor production, 4E cells had decreased cell proliferation in response to hypoxia as determined by BrdU ELISA, a response previously reported in normal fibroblasts (7).

In addition to increased EPO expression in response to anoxia and hypoxia, 4E cells also increased expression of VEGF, another hypoxia-inducible growth factor. Evaluation of cell lysates by Western analysis (Fig. 8A) demonstrated a two- to threefold increase in the cell-associated 43-kDa isoform of VEGF 189 and its 23-kDa cleaved NH₂-terminal fragment (VEGF 121) (13). By ELISA (Table 2), cell-associated VEGF concentrations were over 300-fold higher than EPO and were increased 2-fold by hypoxia. Secreted VEGF was also detectable in cell culture supernatants (data not shown). Western analysis of cell lysates showed that VEGF protein expression

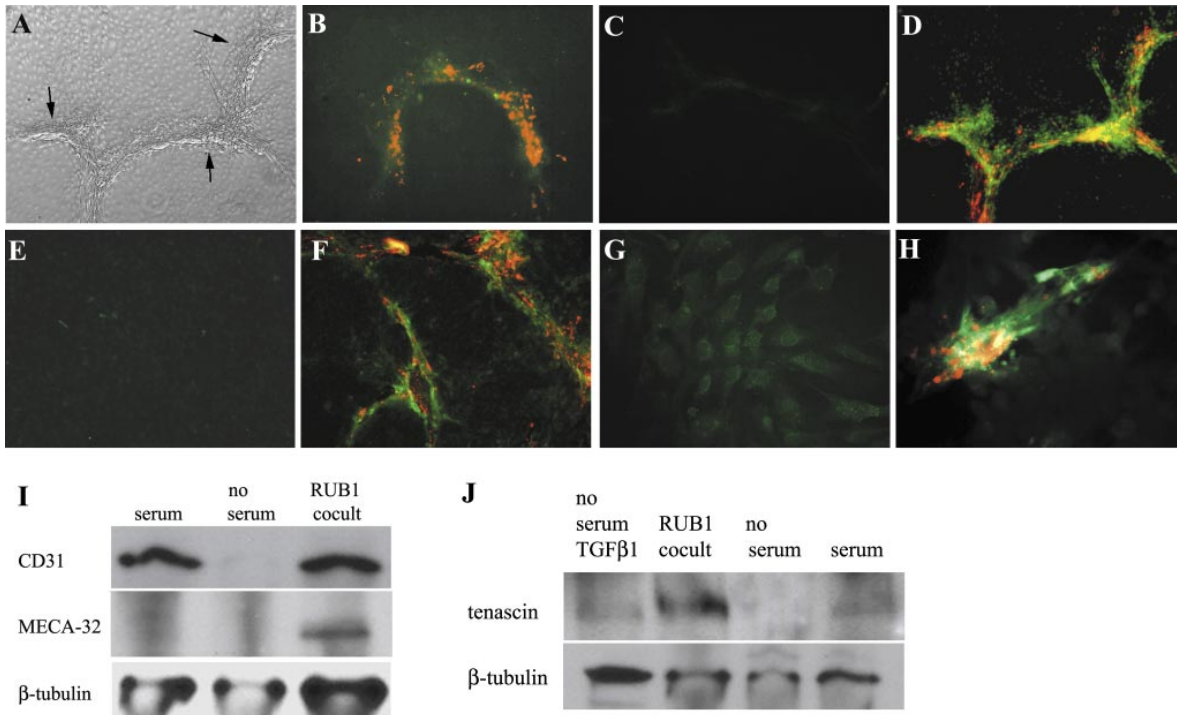


Fig. 4. Coculture with RUB1 ureteric bud cells induced 4E expression of tenascin and an endothelial phenotype. 4E cells were labeled with DiI (red) before coculture. 4E control cells were grown in serum-free medium alone. *A*: phase-contrast image of 4E cell aggregates (arrows) after 1 wk of coculture with RUB1 cells in serum-free medium. 4E aggregates (red) showed no Tie2-GFP signal (*B*). 4E aggregates expressed Flk-1 (*D*) with no expression detected in control cells (*C*). 4E aggregates expressed calponin along their periphery (*F*) with no expression in control cells (*E*). *H*: tenascin expression in 4E aggregates with no tenascin expression in control cells (*G*). Western blot analysis for endothelial markers CD31 and MECA-32 (*H*) demonstrated induction in 4E cells by RUB1 coculture compared with control serum-free cultures. *I*: tenascin expression by Western blot analysis. Coculture with RUB1 cells in serum-free medium induced detectable levels of tenascin while no expression was detected in cells grown in serum-free medium. Addition of TGF- β_1 had an effect equal to growth in serum but less than coculture with RUB1 cells. Original magnification $\times 100$.

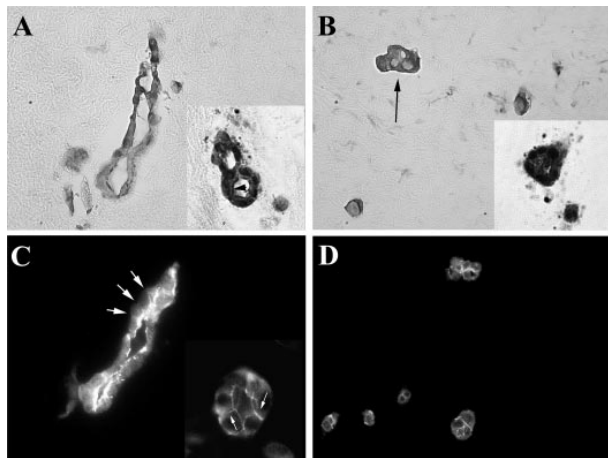


Fig. 5. Coculture of 4E cells with the Madin-Darby canine kidney (MDCK) epithelial cell line. In 3-D type1 collagen gels, tubular structures (*A*, hematoxylin stain, *inset* PAS stain, arrowhead) that expressed the tight junction protein ZO-1 in an apical-lateral location (*C*, arrows and *inset*, arrows) were formed. MDCK cells cultured alone formed cysts (*B*, hematoxylin, *inset* PAS) with nonpolarized ZO-1 expression (*D*). Images are representative of results from 3 separate coculture experiments. Original magnification $\times 400$.

was increased sevenfold by addition of FGF-2 (Fig. 8A), an effect previously reported in stromal cells (4). This was three-fold greater than the response to Shh, an angiogenic morphogen active during embryonic development (30). Double immunostaining for VEGF and EPO demonstrated that VEGF was expressed in the same small (<1%) subset of cells as EPO (Fig. 8B). In contrast, VEGF labeling appeared to be localized to the Golgi network of normoxic cells as previously reported (13) without coexpression of EPO (Fig. 8C).

DISCUSSION

This study demonstrates that multipotent mesenchymal cells with embryonic renal stromal cell characteristics can be cultured from adult kidney. An individual clone (4E) can differentiate into multiple renal interstitial cell types including EPO-producing fibroblasts, pericytes, and endothelial cells and provide paracrine support for both angiogenesis and tubulogenesis. Cells express surface markers found in FVB/NJ mouse bone marrow stromal or mesenchymal stem cells including CD34, Sca-1, and CD44 (28) and genes found specifically in kidney stromal cells during embryonic development including growth factor and cytokine receptors and transcription factors (20). Despite being derived from a single-cell clone, 4E cultures are clearly heterogeneous and likely composed of a mixture of cells including progenitor

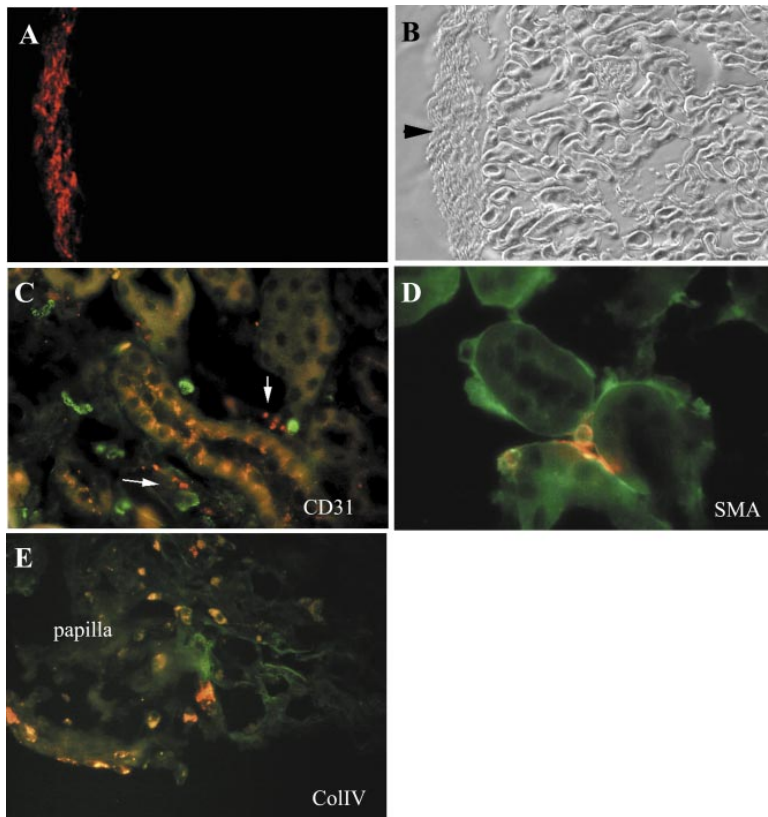


Fig. 6. DiI-labeled 4E cells (red) were injected under the capsule of control (A, B) and ischemic (C-E) kidneys. Tissue was examined after 1 wk of reperfusion. Cells remained in a subcapsular location (arrow) in control kidneys. Following ischemia-reperfusion, cells migrated to peritubular capillaries (C, green: CD31, red: 4E cells, arrows and D, green/yellow: smooth muscle actin), and the periphery of the papilla (E, yellow: type IV collagen signal in 4E cells). Original magnification $\times 100$ (A, B) and $\times 400$ (C-E).

cells and daughter cells at various stages of differentiation along predominately fibroblast or smooth muscle cells lineages. None of the markers studied are individually useful for identifying these cells *in vivo* in the adult kidney as many differentiated cell types express them. It is therefore not possible to prospectively identify these cells within the adult kidney.

The origin of 4E cells remains uncertain. In addition to being derived from resident renal mesenchymal progenitor cells, other possible sources include dedifferentiated fibroblasts or pericytes, circulating MSC sequestered in the kidney either during or after embryonic development, or cells derived from epithelial to mesenchymal *trans*-differentiation that may occur as a result of culture conditions. In a recent study using mice chimeric for labeled bone marrow MSC by bone marrow transplantation and careful detection methods, no evidence that marrow derived stem cells can differentiate into epithelium and contribute to tubular repair following ischemic injury was found. Rare labeled cells however were detected within peritubular capillary endothelium and the interstitium of both control and ischemic kidneys, demonstrating that MSC can migrate and incorporate within the interstitium of the adult kidney (6). Additional evidence for the contribution of bone marrow derived MSC to the interstitial fibroblast population is provided by another study using unilateral ureteral obstruction to cause kidney fibrosis in chimeric mice (14). Following injury, up to 15% of resident fibroblasts in fibrotic tissue were FSP⁺ donor fibroblasts compared with 12% in normal kidneys.

Additional studies of MSC isolated from kidneys of mice with genetically labeled bone marrow MSC, renal epithelial cells, or fibroblasts will be necessary to explore these possibilities.

During kidney development, cells expressing the bHLH transcription factors Pod-1 and BF-2 and the extracellular matrix protein tenascin are located at the cortical medullary junction and later in medullary interstitial cells (5). Stromal progenitor cells expressing these transcription factors differentiate into peritubular interstitial cells of the cortex and medulla and pericytes, supporting the existence of a common progenitor for all stromal cells within the metanephric mesenchyme. Knockout of Pod-1 (31) and BF-2 (10) result in decreased numbers of nephrons and reduced branch elongation of the ureteric bud. The stromal cell factors affecting tubule elongation are unknown but potential mediators include BMP-4 (24) which is expressed by 4E cells. The ability of 4E cells to self-renew and differentiate into multiple interstitial cell types including pericytes, endothelial cells, and 5'-NT-positive, EPO-producing fibroblasts suggests that these cells may function as a multipotent stromal cell progenitor within the adult kidney with similar characteristics as embryonic renal stromal cells.

The functions of the interstitium in the adult kidney remain relatively unknown, in part, due to the assumption that their primary role is production of extracellular matrix. Following injury, conversion of interstitial cells to an embryonic phenotype may support repair of damaged tubules (12). For example, myofibroblasts have been shown to be involved in cellular

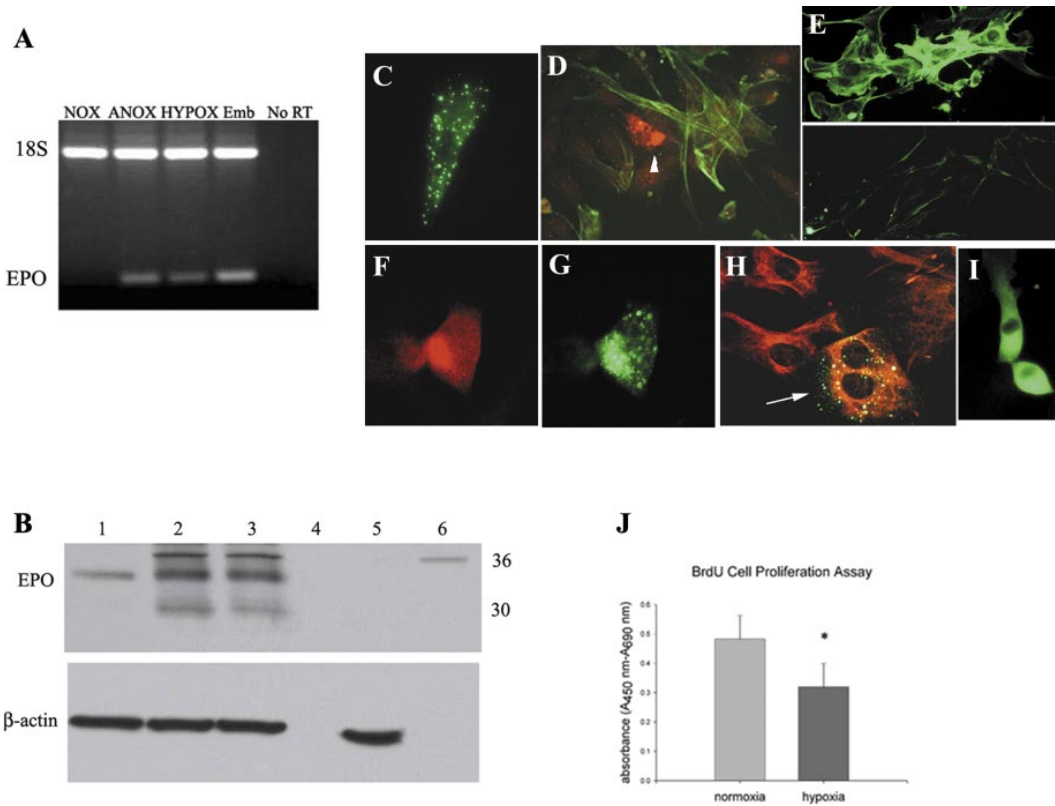


Fig. 7. Expression of EPO in 4E cells grown in normoxic (NOX) hypoxic (HOX, 2% O₂) and anoxic (ANOX, <1% O₂) conditions for 24–48 h. Results presented are representative of at least 3 experiments. **A:** RT-PCR with 18S internal standards: Emb = cDNA from whole E14 mouse embryo, no RT = no added reverse transcriptase. **B:** Western blot analysis of lysates from control NOX cells (lane 1), ANOX cells from 2 separate cultures (lanes 2 and 3) demonstrating expression of 30- and 36-kDa proteins. 3T3 fibroblast lysates used as negative control (lane 5) and recombinant mouse EPO (30 pg) as positive control (lane 6) for 36-kDa EPO protein. β -Actin was used as loading control. Immunocytochemistry using 4E cells cultured in anoxic conditions for 24 h. **C:** EPO labeling of cytoplasmic granules. **D:** EPO positive (red, arrowhead), α -smooth muscle actin negative cell shown next to α -smooth muscle actin positive, EPO negative cells (green). α -smooth muscle actin expression was markedly reduced in anoxic cells (*E, bottom*) compared with controls (*E, top*). Double labeling of ecto-5'-nucleotidase expression (*F*) in EPO-positive cell (*G*). All cells including EPO-positive fibroblasts (arrow) were vimentin positive (*H*). S100A4-positive cells (*I*) were EPO negative and represented <1% of total cell population. Original magnification $\times 400$ (*D-I*) and $\times 600$ (*C*). BrdU ELISA (*J*) demonstrating decreased cell proliferation in response to hypoxia (* $P = 0.0001$).

recovery after uranyl acetate-induced acute renal failure (37). The migration and incorporation of 4E cells into the cortical peritubular interstitium following subcapsular injection after ischemic injury suggest that this cell type participates in renal repair. Loss of the trophic effect of interstitial mesenchymal cells by interstitial fibrosis may account for subsequent loss of the epithelial and endothelial cells that they support and resulting chronic renal failure.

Murine bone marrow stromal cells produce a large number of angiogenic cytokines that may promote arteriogenesis through paracrine mechanisms instead of actual incorporation into the vessel wall (17, 18). Bone marrow MSC have also been reported to differentiate into endothelial cells and con-

Table 2. VEGF and EPO concentrations determined by ELISA

	Normoxia	Anoxia
VEGF, ng[μ l] ⁻¹ [μ g total protein] ⁻¹	2.7 \pm .4	5.8 \pm 0.35
Erythropoietin, pg[μ l] ⁻¹ [μ g total protein] ⁻¹	0	17.0 \pm 1.4

Values represent mean concentrations from 3 experiments \pm SD.

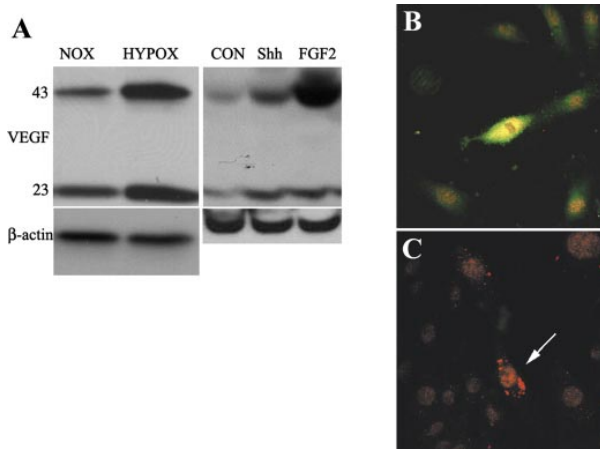


Fig. 8. Double immunolabeling for VEGF (red) and EPO (green) demonstrated dual expression (yellow) in hypoxic cells (*B*) while control cells (*C*, arrow) expressed only VEGF. Western analysis (*A*) for VEGF in normoxic (NOX) and hypoxic (HYPOX) cells demonstrating 3-fold increase in VEGF expression. A 7-fold increase occurred following addition of FGF-2 compared with a 3-fold increase with sonic hedgehog (Shh). β -Actin used as loading control.

tribute to angiogenesis in tumor and ischemic injury models (35). During embryonic development, intrarenal angioblasts are likely to be the precursors for glomerular and peritubular vasculogenesis (1). Peritubular capillary precursors may also exist in adult kidney since capillary proliferation and remodeling occurs following surgical nephron reduction and other renal injury models (29, 32). While previous studies suggested that circulating endothelial cells of bone marrow origin may participate in capillary repair and proliferation, resident progenitors similar to 4E cells may also be involved in angiogenesis in response to renal injury. In response to FGF-2, an angiogenic cytokine, 4E cells increase expression of EPO and VEGF, both well-known angiogenic growth factors. In the hypoxia environment of the Matrigel assay, 4E cells underwent endothelial differentiation and supported capillary formation by forming pericytes. These results suggest that as demonstrated with bone marrow stromal cells, 4E cells may promote angiogenesis by both direct endothelial differentiation and paracrine mechanisms.

4E cells were shown to produce increased amounts of the hypoxia-inducible growth factors VEGF and EPO. VEGF levels were over 300-fold greater than EPO levels, a difference that may be explained by the relatively short half-life and degradation of secreted VEGF. The demonstration of EPO expression establishes 4E cells as the first reported renal fibroblast cell line to produce this hormone. Previous *in vitro* studies of the regulation of EPO expression have relied on tumor cells from the kidney (34) and other organs including liver (8) and brain (36). Similar to EPO-producing cells *in vivo*, this subset of 4E cells also express 5'-NT and are α -SMA negative. With the use of current culture conditions, however, the population of EPO-producing cells is very small and most cells appear to follow alternate pathways such as myofibroblast or smooth muscle differentiation. The relatively low number of EPO-producing cells likely accounts for our inability to detect secreted EPO in culture supernatants. Decreased EPO production following kidney injury may be due to phenotypic conversion of less differentiated fibroblast-like cells to myofibroblasts (22). Given the phenotypic "plasticity" of fibroblasts or their precursors as demonstrated in this study, it is apparent how changes in the peritubular microenvironment following injury may affect EPO production. Future studies using 4E cells may provide additional knowledge about regulation of EPO production in both normal and diseased kidneys. These cells may also be useful for studying the differentiation of EPO-producing fibroblasts from intrarenal precursors, an area of kidney development that has thus far been difficult to investigate. In addition, these cells may also be useful for studying the trophic or support role of the interstitial compartment in both normal kidney homeostasis and following injury.

ACKNOWLEDGMENTS

The authors thank Dr. A. Perantoni for providing RUB-1 cells and Dr. P. Lucas for invaluable assistance in preparing mesenchymal cell cultures.

GRANTS

This work was supported by National Institutes of Health Grants DK-067881 (M. D. Plotkin) and DK-052783 (M. S. Goligorsky).

REFERENCES

1. **Abrahamson DR, Robert B, Hyink DP, St John PL, and Daniel TO.** Origins and formation of microvasculature in the developing kidney. *Kidney Int Suppl* 67: S7–S11, 1998.
2. **Alcorn D, Maric C, and McCausland J.** Development of the renal interstitium. *Pediatr Nephrol* 13: 347–354, 1999.
3. **Baksh D, Song L, and Tuan RS.** Adult mesenchymal stem cells: characterization, differentiation, and application in cell and gene therapy. *J Cell Mol Med* 8: 301–316, 2004.
4. **Claffey KP, Abrams K, Shih SC, Brown LF, Mullen A, and Keough M.** Fibroblast growth factor 2 activation of stromal cell vascular endothelial growth factor expression and angiogenesis. *Lab Invest* 81: 61–75, 2001.
5. **Cullen-McEwen LA, Caruana G, and Bertram JF.** The where, what and why of the developing renal stroma. *Nephron Exp Nephrol* 99: e1–e8, 2005.
6. **Duffield JS, Park KM, Hsiao LL, Kelley VR, Scadden DT, Ichimura T, and Bonventre JV.** Restoration of tubular epithelial cells during repair of the posts ischemic kidney occurs independently of bone marrow-derived stem cells. *J Clin Invest* 115: 1743–1755, 2005.
7. **Gardner L, Li F, Yang X, and Dang C.** Anoxic fibroblasts activate a replication checkpoint that is bypassed by E1a. *Mol Biol Cell* 23: 9032–9045, 2003.
8. **Goldberg MA, Glass GA, Cunningham JM, and Bunn HF.** The regulated expression of erythropoietin by two human hepatoma cell lines. *Proc Natl Acad Sci USA* 84: 7972–7976, 1987.
9. **Hahn AW, Kern F, Jonas U, John M, Buhler FR, and Resink TJ.** Functional aspects of vascular tenascin-C expression. *J Vasc Res* 32: 162–174, 1995.
10. **Hatini V, Huh SO, Herzlinger D, Soares VC, and Lai E.** Essential role of stromal mesenchyme in kidney morphogenesis revealed by targeted disruption of Winged Helix transcription factor BF-2. *Genes Dev* 10: 1467–1478, 1996.
11. **Hay ED.** The mesenchymal cell, its role in the embryo, and the remarkable signaling mechanisms that create it. *Dev Dyn* 233: 706–720, 2005.
12. **Herzlinger D.** Renal interstitial fibrosis: remembrance of things past? *J Clin Invest* 110: 305–306, 2002.
13. **Huez I, Bornes S, Bresson D, Creancier L, and Prats H.** New vascular endothelial growth factor isoform generated by internal ribosome entry site-driven CUG translation initiation. *Mol Endocrinol* 15: 2197–2210, 2001.
14. **Iwano M, Plieth D, Danoff TM, Xue C, Okada H, and Neilson EG.** Evidence that fibroblasts derive from epithelium during tissue fibrosis. *J Clin Invest* 110: 341–350, 2002.
15. **Jones PL and Jones FS.** Tenascin-C in development and disease: gene regulation and cell function. *Matrix Biol* 19: 581–596, 2000.
16. **Karavanova ID, Dove LF, Resau JH, and Perantoni AO.** Conditioned medium from a rat ureteric bud cell line in combination with bFGF induces complete differentiation of isolated metanephric mesenchyme. *Development* 122: 4159–4167, 1996.
17. **Kinnaird T, Stabile E, Burnett MS, Lee CW, Barr S, Fuchs S, and Epstein SE.** Marrow-derived stromal cells express genes encoding a broad spectrum of arteriogenic cytokines and promote *in vitro* and *in vivo* arteriogenesis through paracrine mechanisms. *Circ Res* 94: 678–685, 2004.
18. **Kinnaird T, Stabile E, Burnett MS, Shou M, Lee CW, Barr S, Fuchs S, and Epstein SE.** Local delivery of marrow-derived stromal cells augments collateral perfusion through paracrine mechanisms. *Circulation* 109: 1543–1549, 2004.
19. **Kraal G, Rep M, and Janse M.** Macrophages in T and B cell compartments and other tissue macrophages recognized by monoclonal antibody MOMA-2. An immunohistochemical study. *Scand J Immunol* 26: 653–661, 1987.
20. **Levinson R and Mendelsohn C.** Stromal progenitors are important for patterning epithelial and mesenchymal cell types in the embryonic kidney. *Semin Cell Dev Biol* 14: 225–231, 2003.
21. **Lucas PA, Calcutt AF, Southerland SS, Wilson JA, Harvey RL, Warejcka D, and Young HE.** A population of cells resident within embryonic and newborn rat skeletal muscle is capable of differentiating into multiple mesodermal phenotypes. *Wound Repair Regen* 3: 449–460, 1995.
22. **Maxwell PH, Ferguson DJ, Nicholls LG, Johnson MH, and Ratcliffe PJ.** The interstitial response to renal injury: fibroblast-like cells show

- phenotypic changes and have reduced potential for erythropoietin gene expression. *Kidney Int* 52: 715–724, 1997.
23. **Maxwell PH, Osmond MK, Pugh CW, Heryet A, Nicholls LG, Tan CC, Doe BG, Ferguson DJ, Johnson MH, and Ratcliffe PJ.** Identification of the renal erythropoietin-producing cells using transgenic mice. *Kidney Int* 44: 1149–1162, 1993.
 24. **Miyazaki Y, Oshima K, Fogo A, and Ichikawa I.** Evidence that bone morphogenic protein 4 has multiple biological functions during kidney and urinary tract development. *Kidney Int* 63: 835–844, 2003.
 25. **Montesano R, Schaller G, and Orci L.** Induction of epithelial tubular morphogenesis in vitro by fibroblast-derived soluble factors. *Cell* 66: 697–711, 1991.
 26. **Motoike T, Loughna S, Perens E, Roman BL, Liao W, Chau TC, Richardson CD, Kawate T, Kuno J, Weinstein BM, Stainier DY, and Sato TN.** Universal GFP reporter for the study of vascular development. *Genesis* 28: 75–81, 2000.
 27. **Passaniti A, Taylor RM, Pili R, Guo Y, Long PV, Haney JA, Pauly RR, Grant DS, and Martin GR.** A simple, quantitative method for assessing angiogenesis and antiangiogenic agents using reconstituted basement membrane, heparin, and fibroblast growth factor. *Lab Invest* 67: 519–528, 1992.
 28. **Peister A, Mellad JA, Larson BL, Hall BM, Gibson LF, and Prockop DJ.** Adult stem cells from bone marrow (MSCs) isolated from different strains of inbred mice vary in surface epitopes, rates of proliferation, and differentiation potential. *Blood* 103: 1662–1668, 2004.
 29. **Pillebout E, Burtin M, Yuan HT, Briand P, Woolf AS, Friedlander G, and Terzi F.** Proliferation and remodeling of the peritubular microcirculation after nephron reduction: association with the progression of renal lesions. *Am J Pathol* 159: 547–560, 2001.
 30. **Pola R, Ling LE, Silver M, Corbley MJ, Kearney M, Blake Pepinsky R, Shapiro R, Taylor FR, Baker DP, Asahara T, and Isner JM.** The morphogen Sonic hedgehog is an indirect angiogenic agent upregulating two families of angiogenic growth factors. *Nat Med* 7: 706–711, 2001.
 31. **Quaggin SE, Schwartz L, Cui S, Igarashi P, Deimling J, Post M, and Rossant J.** The basic-helix-loop-helix protein pod1 is critically important for kidney and lung organogenesis. *Development* 126: 5771–5783, 1999.
 32. **Rosenberger C, Griethe W, Gruber G, Wiesener M, Frei U, Bachmann S, and Eckardt KU.** Cellular responses to hypoxia after renal segmental infarction. *Kidney Int* 64: 874–886, 2003.
 33. **Sabatini F, Petecchia L, Tavian M, de Villeroche VJ, Rossi GA, and Brouty-Boye D.** Human bronchial fibroblasts exhibit a mesenchymal stem cell phenotype and multilineage differentiating potentialities. *Lab Invest* 85: 962–971, 2005.
 34. **Sherwood JB and Shouval D.** Continuous production of erythropoietin by an established human renal carcinoma cell line: development of the cell line. *Proc Natl Acad Sci USA* 83: 165–169, 1986.
 35. **Silva GV, Litovsky S, Assad JA, Sousa AL, Martin BJ, Vela D, Coulter SC, Lin J, Ober J, Vaughn WK, Branco RV, Oliveira EM, He R, Geng YJ, Willerson JT, and Perin EC.** Mesenchymal stem cells differentiate into an endothelial phenotype, enhance vascular density, and improve heart function in a canine chronic ischemia model. *Circulation* 111: 150–156, 2005.
 36. **Stolze I, Berchner-Pfannschmidt U, Freitag P, Wotzlaw C, Rossler J, Frede S, Acker H, and Fandrey J.** Hypoxia-inducible erythropoietin gene expression in human neuroblastoma cells. *Blood* 100: 2623–2628, 2002.
 37. **Sun DF, Fujigaki Y, Fujimoto T, Yonemura K, and Hishida A.** Possible involvement of myofibroblasts in cellular recovery of uranyl acetate-induced acute renal failure in rats. *Am J Pathol* 157: 1321–1335, 2000.
 38. **Togel F, Hu Z, Weiss K, Isaac J, Lange C, and Westenfelder C.** Administered mesenchymal stem cells protect against ischemic acute renal failure through differentiation-independent mechanisms. *Am J Physiol Renal Physiol* 289: F31–F42, 2005.
 39. **Young HE, Mancini ML, Wright RP, Smith JC, Black AC Jr, Reagan CR, and Lucas PA.** Mesenchymal stem cells reside within the connective tissues of many organs. *Dev Dyn* 202: 137–144, 1995.

